RJC

RASĀYAN *J. Chem.*
Vol. 14 | No. 1 |389-396| January - March | 2021
ISSN: 0974-1496 | e-ISSN: 0976-0083 | CODEN: RJCABP
http://www.rasayanjournal.com
http://www.rasayanjournal.co.in

VIBRATIONAL SPECTROSCOPIC INVESTIGATION AND ELECTRONIC PROPERTIES OF 4-HYDROXY-3-METHYLBENZOIC ACID

Palanimurugan[1] and S. Jeyavijayan[2,✉]

[1]Department of Physics, Dr. B.R. Ambedkar Institute of Technology, Port Blair-744103, Andaman & Nicobar Islands, India

[2]Department of Physics, Kalasalingam Academy of Research and Education, Krishnankoil-626 126, Tamil Nadu, India

✉Corresponding Author: sjeyavijayan@gmail.com

ABSTRACT

The vibrational spectra for 4-hydroxy-3-methylbenzoic acid (HMBA) were recorded using FT-Raman (3600–100 cm^{-1}) as well as FTIR (4000-400 cm^{-1}) spectroscopies and the assignment of normal modes of the molecule was subsequently established by total energy distributions (TEDs). The density functional theory (DFT) calculations have been performed and compared through the wavenumbers of the observed results. The slight changes among the observed and computed wavenumbers indicate the ability of the computational method used in this study. The HOMO-LUMO charge-transfer interactions of the molecule which are the key factor for biological activity have been discussed. Further, the electronic properties of the molecule have been examined by Mulliken's charge and molecular electrostatic potential (MEP) studies.

Keywords: FTIR, FT-Raman, DFT, 4-hydroxy-3-methylbenzoic acid, MEP

RASĀYAN *J. Chem.*, Vol. 14, No.1, 2021

INTRODUCTION

Benzoic acid derivatives have been attracted towards many biomedical properties such as antiviral, antioxidant, antitumor, antifungal, antimicrobial, anti-inflammatory, radical regulating, hepatoprotective and cytoprotective effects.[1-3] They are also used in identifying fibrotic skin disorder, gastrointestinal disorder and in the medication of drug against ultraviolet radiation[4]. Recently, the motivating features of benzoic acid derivatives have pulled many researchers to take up research in the field of spectroscopy.[5-7] More recently, the spectroscopic properties of metronidazole metal complexes with benzoic acid derivatives have been investigated by Tella et al.[8] However, the survey on literature exposes that the spectroscopic investigations of 4-hydroxy-3-methylbenzoic acid (HMBA) along with the DFT calculation have not been reported. Hence, in the present investigation, DFT-based quantum chemical calculations for optimized parameters and wavenumbers are calculated and the performance of the B3LYP/6-311++G(d,p) computational method is matched with the experimental results.

EXPERIMENTAL

The FTIR spectra of HMBA were recorded in the region 4000–400 $cm^{-1}$with the aid of a Perkin Elmer FTIR spectrometer furnished with an MCT detector, globar source and a KBr beam splitter. The resolution of the spectrum is ±1 cm^{-1}. The computer-based BRUKER RFS-66V model interferometer has been used for recording the FT-Raman spectrum of HMBA in the region (3600–100 cm^{-1}) by Nd: YAG laser source working at 1064 nm wavelength with 200 mW power.

DFT Calculations

Density functional calculations for HMBA have been carried out by using GAUSSIAN suite program[9] through Becke-3-Lee-Yang-Parr (B3LYP) functional[10,11] augmented with larger basis set (6-311++G(d,p)). All the factors involved in the calculations of molecular geometrical parameters, frequencies and electronic parameters were allowed to converge for an optimized geometry of the

http://dx.doi.org/10.31788/ RJC.2021.1415896

molecule and a better agreement was obtained between computational and experimental data. The scaling of computed wavenumbers and total energy distribution (TED) calculation has been performed by the MOLVIB program.[12]

RESULTS AND DISCUSSION

Molecular Geometry

The optimized structure of HMBA is revealed in Fig.-1. The molecule has carboxylic, hydroxyl and methyl groups attached with the benzene ring. The FTIR and FT-Raman spectra of HMBA are represented in Figs.-2 and 3, respectively. The calculated parameters along with experimental results for HMBA are presented in Table-1. The minimum energy and dipole moment for HMBA by the DFT/B3LYP/6-311++G(d,p) optimization is found as -535.52558325 Hartrees and 2.190 Debye, respectively. The hydroxyl, carboxylic and methyl group substitutions in the position of H atoms distort the ring system slightly and bond angle alterations from the perfect planar structure. The C–C experimental[13] bond length order in the ring are C4–C5 < C3–C4 < C6–C1 < C2–C3 = C5–C6 < C1–C2. But, from the B3LYP/6-311++G (d,p) calculated results, the bond length order is somewhat varied as C5–C6 < C2–C3 < C4–C5 < C6–C1 < C1–C2 < C3–C4, meanwhile the phases are dissimilar. Further, the ring looks to be imbalanced because of the C2–C1 and C4–C3 bond lengths at the substitution place, which are calculated as 1.402 and 1.407 Å. These are longer than the remaining C-C bonds in the ring. The computed bond angles C2–C1–C6, C2–C3–C4 and C3–C4–C5 are found as 119.13°, 117.51° and 121.28°, respectively, and are diverged from the regular plane angle of 120°. This asymmetry reveals the repulsion between COOH, CH_3, OH groups and the HMBA ring system.

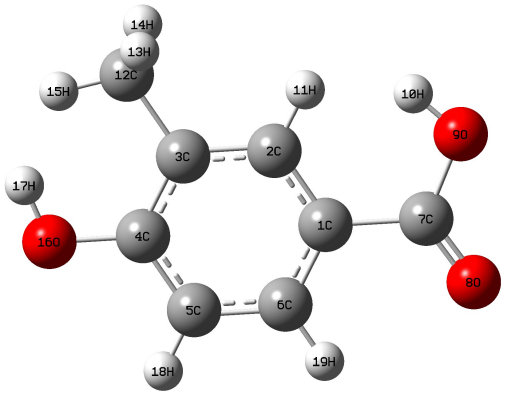

Fig.-1: Optimized Structure of 4-hydroxy-3-methylbenzoic Acid

Table-1: Optimized Geometrical Parameters for 4-hydroxy-3-methylbenzoic Acid

Bond Length	Value (Å) B3LYP/ 6-311++G(d,p)	[13]Expt	Bond Angle	Value (°) B3LYP/ 6-311++G(d,p)	[13]Expt
C1-C2	1.402	1.433	C2-C1-C6	119.31	117.9
C1-C6	1.398	1.395	C2-C1-C7	118.35	118.5
C1-C7	1.479	1.414	C6-C1-C7	122.34	123.6
C2-C3	1.389	1.413	C1-C2-C3	122.03	121.9
C2-H11	1.084	-	C1-C2-H11	118.25	-
C3-C4	1.407	1.368	C3-C2-H11	119.73	-
C3-C12	1.506	1.515	C2-C3-C4	117.51	118.5
C4-C5	1.396	1.361	C2-C3-C12	122.25	122.8
C4-O16	1.365	1.365	C4-C3-C12	120.24	118.5
C5-C6	1.389	1.413	C3-C4-C5	121.28	121.9
C5-H18	1.086	-	C3-C4-O16	116.69	118.5
C6-H19	1.082	-	C5-C4-O16	122.03	120.2

C7=O8	1.211	1.275	C4-C5-C6	120.11	120.7
C7-O9	1.362	1.309	C4-C5-H18	119.78	-
O9-H10	0.968	-	C6-C5-H18	120.11	-
C12-H13	1.094	-	C1-C6-C5	119.76	118.5
C12-H14	1.091	-	C1-C6-H19	120.05	-
C12-H15	1.040	-	C5-C6-H19	120.18	-
O16-H17	0.963	-	C1-C7-O8	125.39	123.5
			C1-C7-O9	113.08	114.5
			O8-C7-O9	121.52	115.5
			C7-O9-H10	106.42	-
			C3-C12-H13	111.19	-
			C3-C12-H14	110.67	-
			C3-C12-H15	111.19	-
			H13-C12-H14	108.48	-
			H13-C12-H15	106.68	-
			H14-C12-H15	108.48	-
			C4-O16-H17	110.00	-

Vibrational Assignment

HMBA consists of 19 atoms which lead 51 normal modes agreeing with C_1 point group. The assignment of vibrational modes for HMBA together with the computed Raman, IR frequencies, intensities, reduced mass and force constants are reported in Table-2. The approximate treatment for correlations of electrons and anharmonicity in the DFT calculations, which creates a discrepancy between observed and calculated wavenumbers. These are corrected by proper scaling of frequencies. Therefore, the scale factor of 0.9613 was utilized in the scaling of calculated frequencies for B3LYP method.[14]

O-H Vibrations

The O-H group in any ring system appears with band broadening and larger intensity and reduces the band to 3200–3550 cm^{-1} regions[15]. Thus, the stretching vibrations of OH group in HMBA are detected at 3285, 3231 cm^{-1} in IR spectrum, which is further confirmed by their TED (almost 100%). The in-plane O-H bending vibration is commonly found between 1440 and 1260 cm^{-1} due to the strong intermolecular interaction. Hence, the band at 1437 cm^{-1} in IR and Raman spectra at 1370 cm^{-1} are allocated to the in-plane O-H deformation of HMBA and these are mixed deeply with other molecular vibrations. In this study, the out-of-plane O-H bending modes of HMBA are also observed and are listed in Table-2.

C-H Vibrations

In the benzene derivatives, the vibrations for C-H stretching[16] are usually occurred in the region 3100–3000 cm^{-1}, because of the unaffected nature of these bands due to the different substituents. In this study, the Raman bands found at 3077, 3058, 2982 cm^{-1} then the FTIR band at 2980 cm^{-1} are designated to stretching C-H vibrations, which contributed to the maximum value of TED. The bands due to C-H in-plane vibrations are found in the 1300–1000 cm^{-1} region and the out-of-plane C-H deformation are powerfully tied with the ring system. In HMBA, the in-plane C–H bending vibrations are detected at 1145, 1109 cm^{-1} in FT-Raman and 1142, 1108, 1039 cm^{-1} in the FTIR spectrum. From Table-2, the B3LYP/6-311++G(d,p) results and the experimental values for C-H vibrational modes are in excellent agreement.

CH_3 Vibrations

CH_3 group vibrations are usually electron-donors in the aromatic ring systems. The asymmetric and symmetric stretching modes of CH_3 group[17] is appeared around the region 2980 and 2870 cm^{-1},

respectively. In this study, the active IR band at 2955 cm^{-1} is attributed to stretching CH_3 in-plane vibration with 95% TED contribution. In HMBA, the Raman band found at 2927 cm^{-1} has been assigned to CH_3 symmetric stretching. For CH_3 substituted derivatives[17], the symmetric and antisymmetric deformation modes of CH_3 group generally occur in the regions 1390-1370 cm^{-1} and 1465-1440 cm^{-1}, respectively. Thus, in HMBA, IR band at 1470 cm^{-1} is allocated to CH_3 in-plane bending vibration and the band at 1378 cm^{-1} has been consigned to CH_3 symmetric bending. The remaining CH_3 vibrational modes are also in noble agreement with the calculated B3LYP/6-311++G(d,p) results and are given in Table-2.

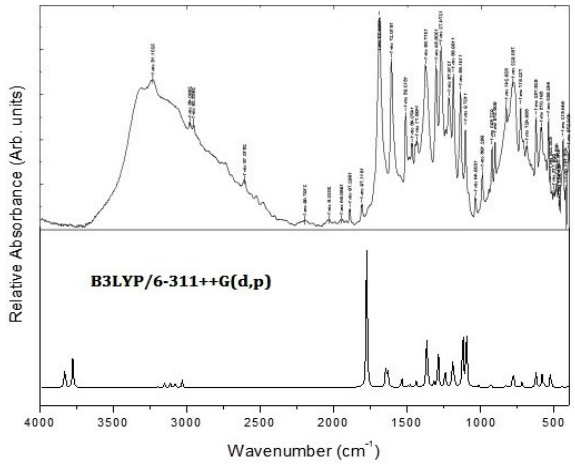

Fig.-2: FTIR Spectra of HMBA

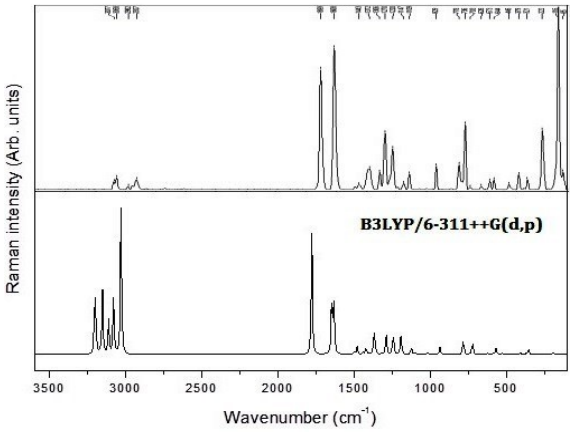

Fig.-3: FT-Raman Spectra of HMBA

COOH Vibrations

The carboxylic group stretching vibration[17] is typically detected in the range 1690-1655 cm^{-1}. The FTIR and FT-Raman bands that appeared at 1692 and 1695 cm^{-1} in HMBA have been consigned to C=O stretching. The experimental bands at 927 and 445 cm^{-1} are attributed to in-plane and out-of-plane C=O bending vibrations, respectively, for HMBA, which are in agreement with the similar literature reports[18]. The wavenumbers of C–O group have been the focus of extensive studies since they have the typical bands in the ketons spectra[18] and are expected in the region 1350–1200 cm^{-1}. The in-plane O–H bending and stretching C–O vibrations of HMBA are also assigned and given in Table-2.

C-C Vibrations

In benzene derivatives, the bands in the range 1430-1625 cm^{-1} are owing to C-C stretching vibrations[19]. Thus, the stretching C-C modes of HMBA are found at 1610, 1514, 1479, 1307, 1219, 1190 cm^{-1} in the FTIR and 1608, 1488, 1443, 1306, 1220 cm^{-1} in the FT-Raman. These modes are proven by their TED percentage. The in-plane C-C-C deformation bands arise in the 1000–600 cm^{-1} region. In the current study, the ring bending modes are assigned by careful attention to numerical descriptions of HMBA. The maximum % of TED acquired for these vibrations promising and approves the assignments made for HMBA. The ring out-of-plane deformations are also enumerated in Table-2.

Mulliken Atomic Charges

The role played by the atomic charges in the molecular systems is very important in the quantum chemical calculations[20]. The results obtained for HMBA show that the different substitution groups in the ring evidence the reallocation of electron density. The C1, C3 carbon atoms have positive charges (1.321 and 0.426) and C4 has the negative (-1.639) charge as exposed in Fig.-4. This is because of the addition of COOH, CH_3 and OH groups in the ring. The hydrogen atom (H17) has a charge of 0.2625 due to bound with a more electronegative oxygen atom (O16) of the hydroxyl group. The charge distribution of HMBA is balanced by the electron-withdrawing and electron-donating groups attached with the atoms C1, C3 and C4, respectively.

Table- 2: Vibrational Assignments (Characterized by TED) for 4-hydroxy-3-methyl benzoic Acid along with Calculated IR Intensity (km/mol), Raman Activity (Å amu^{-1}), Reduced Mass (amu) and Force Constant (m dyne A^{-1}) based on DFT Method

S. No.	Observed Wavenumber (cm^{-1})		Calculated Wavenumber (cm^{-1}) B3LYP/6-311++G(d,p)						Assignment (TED %)
	FTIR	FT-Raman	Unscaled	Scaled	Reduced mass	Force Constant	IR intensity	Raman activity	
1	3285(s)	-	3829	3681	6.14	13.46	91.91	1.10	νOH (99)
2	3231(vs)	-	3775	3629	5.61	23.76	241.52	1.04	νOH (98)
3	-	3077(vw)	3211	3087	17.83	415.80	143.27	9.57	νCH (98)
4	-	3058(w)	3189	3066	9.21	3.88	148.64	1.10	νCH (96)
5	2980(w)	2982(vw)	3153	3031	8.94	164.89	144.05	4.66	νCH (97)
6	2955(w)	-	3114	2993	6.64	342.69	85.03	8.07	CH_3 ips (95)
7	-	2927(w)	3079	2960	6.54	0.99	57.01	3.30	CH_3 ss (94)
8	2610(w)	-	3031	2914	6.39	2.24	113.67	3.18	CH_3 ops (96)
9	1692(vs)	1695(vs)	1778	1709	6.70	159.54	56.75	5.63	νC=O (93)
10	1610(vs)	1608(vs)	1645	1581	9.75	94.40	3.73	1.62	νCC (84), bCC (13)
11	1514(s)	-	1630	1567	9.63	117.07	23.59	4.42	νCC (85), bCH (12)
12	-	1488(vw)	1536	1477	3.63	85.32	30.74	5.47	νCC (81), Rasymd (15)
13	1479(vw)	-	1499	1441	1.73	8.09	9.99	4.81	νCC (80), CC (17)
14	1470(ms)	-	1480	1423	1.35	6.70	0.91	3.77	CH_3 ipb (89)
15	-	1443(w)	1450	1394	3.58	69.39	21.23	5.45	νCC (79), bCC (19)
16	1437(ms)	-	1420	1365	1.49	143.81	2.43	1.31	bOH (79), bCO (15)
17	1378(s)		1371	1318	3.75	9.96	8.56	1.40	CH_3 sb (78)
18	-	1370(ms)	1359	1306	2.88	60.62	13.49	5.41	bOH (80), bCC (17)
19	1307(s)	1306(ms)	1314	1263	0.70	12.44	0.04	1.88	νCC (77), CC (21)
20	1275(s)	-	1289	1239	0.73	11.33	0.05	3.02	νCO (82)
21	-	1269(s)	1242	1194	2.74	43.91	9.94	5.13	νCO (81)
22	1219(ms)	1220(s)	1187	1141	1.57	47.12	4.93	1.72	νCC (80), Rtrigd (15)
23	1190(s)	-	1179	1133	3.43	1.88	17.64	4.64	νCC (74), Rsymd (17)
24	1142(s)	1145(w)	1135	1091	2.00	25.18	9.63	3.77	bCH (68), Rasymd (21)
25	1108(ms)	1109(ms)	1108	1065	1.03	8.29	11.79	1.23	bCH (63), CC (23)
26	1039(w)	-	1064	1023	1.42	7.99	0.43	9.19	bCH (65), Rtrigd (19)
27	992(ms)	-	1014	975	1.67	15.10	5.82	3.34	CH_3 opb (80)
28	927(ms)	927(ms)	952	915	0.69	0.05	2.44	1.31	bC=O (73), bCC (13)
29	906(ms)	-	941	905	1.66	7.41	0.05	1.04	CH_3 ipr (71)
30	829(w)	-	927	891	1.35	13.54	1.58	2.89	Rtrigd (70), Rsymd (19)
31	783(ms)	-	823	791	1.49	1.62	1.26	1.25	Rasymd (72), CC (21)
32	-	778(ms)	779	749	1.13	15.27	4.69	3.38	CH_3 opr (70)
33	732(ms)	736(s)	778	748	1.24	13.18	1.21	2.64	bCO (71), bCC (15)
34	-	703(vw)	723	695	1.70	95.59	1.92	6.11	bCO (72), bCC (13)
35	689(w)	-	712	684	1.00	1.42	0.10	6.15	Rsymd (69), Rasymd (21)
36	627(ms)	628(vw)	620	596	0.94	8.92	1.16	2.61	bCC (65), CC (23)
37	591(ms)	-	583	560	0.32	49.19	1.69	1.54	bCC (60), Rtrigd (19)
38	-	573(w)	560	538	0.82	0.88	4.34	3.50	ωOH (59), ωCC (23)
39	543(ms)	544(w)	540	519	0.94	6.05	0.48	2.20	ωOH (59), tRtrig (24)
40	530(w)	-	523	503	0.30	43.87	116.12	1.24	ωCH (57), bCC (15)
41	509(w)	-	448	431	0.36	30.09	22.82	1.73	ωCH (55), tRtrig (27)
42	485(w)	-	406	390	0.50	1.00	0.39	2.19	ωCH (60), ωCC (19)
43	470(w)	-	360	346	0.09	4.12	0.70	2.34	ωCC (53), ωCO (23)

44	462(w)	-	351	337	0.67	6.27	1.42	1.50	ωCC (55), tRasym (23)
45	445(w)	445(w)	305	293	0.18	0.91	0.24	1.56	ωC=O (51), ωCC (23)
46	426(w)	-	291	280	0.17	82.21	0.04	1.09	tRtrig (53), tRsym (27)
47	404(ms)	399(ms)	190	183	0.07	103.93	16.69	1.09	tRasym (51), ωCO (21)
48	-	321(w)	179	172	0.11	0.87	0.23	1.10	ωCO (52), tRtrig (19)
49	-	222(s)	130	125	0.01	0.01	0.30	1.07	ωCO (55), tRtrig (19)
50	-	116(vs)	106	102	0.03	0.11	0.35	1.06	tRsym (51), tRasym (21)
51	-	85(w)	62	60	0.02	0.77	0.01	1.09	tCH_3 (63)

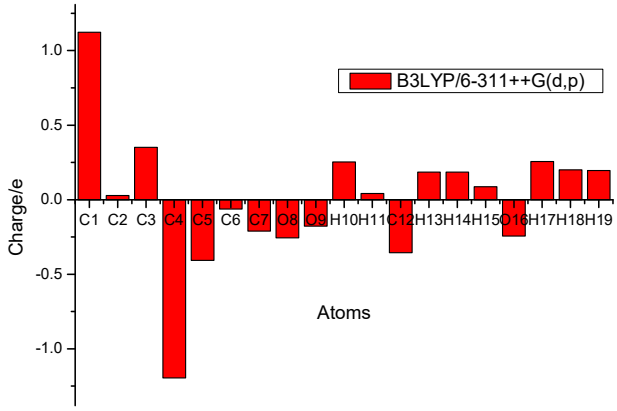

Fig.-4: Mulliken's Plot for 4-hydroxy-3-methylbenzoic Acid

HOMO-LUMO Bandgap

The chemical stability of any molecule can be decided by both the lowest unoccupied and highest occupied molecular orbitals[21] (LUMO and HOMO). The HOMO and LUMO signify the capability of the molecule to donate and accept an electron, respectively. The frontier molecular orbitals computed by B3LYP/6-311G++(d,p) level for HMBA are elucidated in Fig.-5. The HOMO and LUMO energy gap for HMBA is found to be 5.209 eV, which explicates the charge-transfer interactions of the molecule. The HOMO is located over the -OH group, LUMO is sited over the benzene ring and COOH group. Therefore, the HOMO-LUMO transition clarifies that the electron density is transferred from the hydroxyl group to the aromatic ring and COOH assembly.

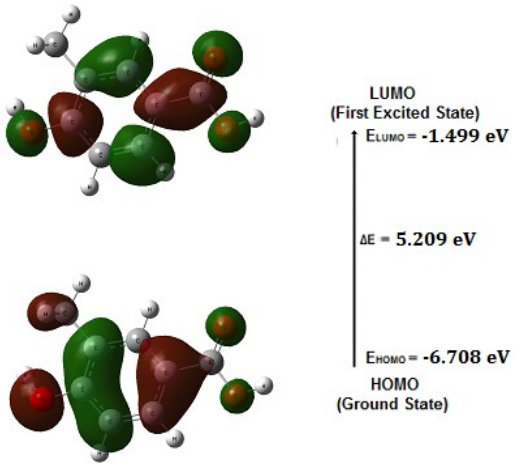

Fig.-5: HOMO-LUMO Plot for 4-hydroxy-3-methylbenzoic Acid

Molecular Electrostatic Potential

The electrostatic potential has been employed for calculating comparative reactivities to nucleophilic and electrophilic attacks and in the examination of hydrogen bonding interactions and biological recognition[22]. In this investigation, the B3LYP/6-311++G(d,p) calculated the electrostatic potential for HMBA is presented in Fig.-6. The MEP map demonstrations that the oxygen atoms (Red) of OH and COOH groups specify the site of negative potential and the hydrogen atoms (Blue) of these groups represent the positive potential site region. This result states that the oxygen atoms designate the strongest repulsion and H atoms to show the strongest attraction. Thus, the HMBA displays the maximum reactive regions for electrophilic and nucleophilic attacks.

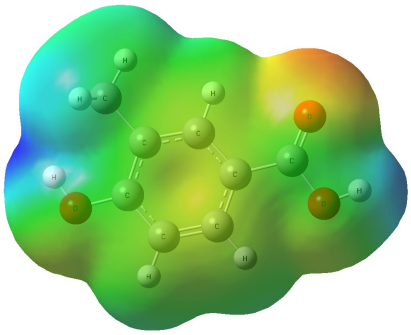

Fig.-6: Molecular Electrostatic Potential (MEP) for 4-hydroxy-3-methylbenzoic Acid

CONCLUSION

The vibrational spectra such as FT-Raman and FTIR for 4-hydroxy-3-methylbenzoic acid have been studied based on the scaled DFT/B3LYP method with a larger basis set. The calculated optimized parameters, frequencies of normal modes are compared with the experimental results and are found to be unambiguous. The effects of carboxylic, hydroxyl and methyl groups involved in the ring have been investigated. The molecular charge-transfer interactions and electronic properties of the molecule are conferred with the help of Mulliken's charge and HOMO-LUMO analyses. Furthermore, the nucleophilic and electrophilic attacks of the molecule have been examined through the molecular electrostatic potential.

REFERENCES

1. O.G. Bountagkidou, S.A. Ordoudi, M.Z. Tsimidou, *Food Research International*, **43**, 2014(2010), **DOI:**10.1016/j.foodres.2010.05.021
2. T. Tanaka, T. Tanaka, M. Tanaka, *Journal of Experimental & Clinical Medicine*, **3**, 27(2011), **DOI:**10.1016/j.jecm.2010.12.005
3. Y.G. Cao, L. Zhang, C. Ma, B.B. Chang, Y.C. Chen, Y.G. Tang, X.D. Liu, X.Q. Li, *Biochemical Pharmacology*, **77**, 1096(2009), **DOI:**10.1016/j.bcp.2008.11.029
4. R. Swinslocka, M. Samsonowicz, E. Regulaska, W. Lewandowski, *Journal of Molecular Structure*, **792**, 227(2006), **DOI:**10.1016/j.molstruc.2005.10.060
5. G.B. Tolstorozhev M.V. Belkov, I.V. Skornyakov, O.K. Bazyl, V.Ya. Artyukhov, G.V. Mayer, O.I. Shadyro, P.V. Kuzovkov, S.D. Brinkevich and S.N. Samovich, *Journal of Applied Spectroscopy*, **81**, 109(2014), **DOI:**10.1007/s10812-014-9895-8
6. M. Kurt, E. Babur Sas, M. Can, S. Okur, S. Icli, S. Demic, M. Karabacak, T. Jayavarthanan, N. Sundaraganesan, *Spectrochimica Acta Part A: Molecular and Biomolecular Spectroscopy*, **152**, 8(2016), **DOI:**10.1016/j.saa.2015.07.058
7. S. Pramanik, T. Dey, A.K. Mukherjee, *Journal of Molecular Structure*, **1175**, 185(2019), **DOI:**10.1016/j.molstruc.2018.07.090
8. A.C. Tella, N.J. Shamle, J.A. Obaleye, A.C. Whitwood, S.A. Bourne, P.A. Ajibade, *Journal of Molecular Structure*, **1209**, 127925(2020), **DOI:**10.1016/j.molstruc.2020.127925
9. M.J. Frisch et al. GAUSSIAN 09, Revision A.02, Gaussian Inc, Wallingford CT, (2009).

10. A.D. Becke, *The Journal of Chemical Physics*, **98**, 5648(1993), **DOI:**10.1063/1.464913
11. C. Lee, W. Yang, R.G. Parr, *Physical Review*, **37**, 785(1988), **DOI:**10.1103/PhysRevB.37.785
12. MOLVIB (V.7.0): *Calculation of Hormonic Force Fields and Vibrational Modes of Molecules*, QCPE program No.807, (2002).
13. M.P. Gupta, S.M. Prasad, *Acta Crystallographica*, **27B**, 713(1971), **DOI:**10.1107/S0567740871002814
14. D.C. Young, *Computional Chemistry: A Pratical Guide for Applying Techniques to Real-World Problems*, John Wiley & Sons, Inc., New York, (2001).
15. D. N. Sathyanarayana, *Vibrational Spectroscopy Theory and Applications*, second ed., New Age International (P) Limited Publishers, New Delhi, (2004).
16. L. Usha Kumari, M. Fathima Beegum, B. Harikumar, H. T. Varghese, C. Yohannan Panicker, *Rasayan Journal of Chemistry,* **1**, 246(2008).
17. E. Gobinath, *S.* Jeyavijayan, R. John Xavier, *Indian Journal* of *Pure & Applied Physics***, 55**, 541(2017).
18. S. Jeyavijayan, *Spectrochimica Acta Part A: Molecular and Biomolecular Spectroscopy*, **136**, 553(2015), **DOI:**10.1016/j.saa.2014.09.069
19. T.Chithambarathanu, K.Vanaja, J. Daisy Magdaline, Rasayan Journal of Chemistry, **8(4)**, 490(2015).
20. V.K. Rastogi, M.A. Palafox, L. Mittal, N. Peica, W. Kiefer, K. Lang, P. Ohja, *Journal of Raman Spectroscopy*, **38,** 1227(2007), **DOI:**10.1002/jrs.1725
21. S. Jeyavijayan, Palanimurugan, K.Viswanathan, V. Lavanya , K. Gurushankar, *Rasayan Journal of Chemistry*, **12(2)**, 921(2019), **DOI:**10.31788/RJC.2019.1225156
22. J.S. Murray, K. Sen, *Molecular Electrostatic Potentials, Concepts and Applications*, Elsevier, Amsterdam, pp. 7-624, (1996).

[RJC-5896/2020]